Polymer 51 (2010) 3926–3933

Contents lists available at ScienceDirect

Polymer

journal homepage: www.elsevier.com/locate/polymer

Engineering oligo(ethylene glycol)-based thermosensitive microgels for drug delivery applications

Ting Zhou, Weitai Wu, Shuiqin Zhou*

Department of Chemistry of College of Staten Island, and The Graduate Center, The City University of New York, 2800 Victory Boulevard, Staten Island, New York 10314, USA

ARTICLE INFO

Article history:
Received 3 May 2010
Received in revised form
12 June 2010
Accepted 15 June 2010
Available online 22 June 2010

Keywords:
PEG
Microgel
Drug delivery

ABSTRACT

Novel oligo(ethylene glycol)-based thermosensitive microgels with well engineered core-shell structures were developed for storage and delivery of chemotherapeutic agents. The core is consisted of hydrophobic poly[2-(2-methoxyethoxy)ethyl methacrylate], while the shell is consisted of hydrophilic copolymer of 2-(2-methoxyethoxy)ethyl methacrylate with oligo(ethylene glycol) methyl ether methacrylates. These core-shell microgels exhibit tunable volume phase transition temperature and excellent colloidal stability across the physiologically important temperature range. The thickness of the hydrophilic shell can control the collapsing degree (or mesh size) of the hydrophobic core network, which can be utilized to significantly increase the loading capacity of the model hydrophobic drugs dipyridamole by tailoring the shell thickness of microgels. While the microgels are nontoxic, the drug molecules released from the microgels remain active to kill the cancer cells. The presented results provide important guidelines for the rational design of core-shell structured polymeric microgels for drug uptake and release applications.

1. Introduction

Microgel particles as drug delivery carriers for biological and biomedical applications have received increasing attention during the last decade due to their unique chemical and physical versatility [1–6]. Microgels offer several advantages over other polymer based drug delivery systems: simple synthesis, tunable size from nanometers to micrometers, large surface area for effective bioconjugation to add target ligands for site-specific delivery, an interior network structure for the incorporation of drug molecules to protect the drug from hydrolysis and other type of chemical degradation, and potential biocompatibility. Among the various approaches used to enhance the efficacy of chemotherapy is the use of smart carrier systems that can release a drug in response to stimuli, such as changes in pH, temperature, light, or the presence of specific enzymes that are selectively encountered in relevant cell organelles [7–10].

So far, the thermo-responsive poly(*N*-isopropylacrylamide) (PNIPAM)-based microgels have been most extensively studied for applications in drug delivery [8–21], including the introduction of other environmental sensitivities such as pH, glucose, and light sensitive components into the PNIPAM microgels to control the drug release. However, the well studied PNIPAM-based microgels have not been translated into a biomedical breakthrough although a recent study on the microgels containing NIPAM and acrylic acid (AA) indicated no adverse effects [16]. To meet the general requirement in biocompatibility of the materials used for drug delivery systems, an important challenge is to develop biocompatible polymers which have similar properties to PNIPAM [4]. Thermo-responsive polymers containing short oligo(ethylene glycol) side chains were recently proposed as an attractive alternative to PNIPAM [22–28]. The lower critical solution temperature (LCST) of these graft polymers are tunable through the control in the compositions of the oligo(ethylene glycol) side chains. Lutz et al. have reported that the LCST of the copolymers composed of 2-(2-methoxyethoxy)ethyl methacrylate (MEO_2MA) with oligo (ethylene glycol) methyl ether methacrylate (M_n = 475 g/mol, MEO_9MA) can be adjusted by varying the comonomer ratios [22–24]. Ishizone et al. found that the LCST of the poly[oligo (ethylene glycol) alkyl ether methacrylates] is tunable by varying the oligo(ethylene glycol) side chain length [26,27]. The longer the oligo(ethylene glycol) side chain, the higher the LCST of the graft polymer. In addition, the star-block copolymers of these oligo (ethylene glycol) methyl ether methacrylate with star poly (ethylene glycol) (PEG) exhibit thermoreversible sol-gel transitions in physiological media [28]. Although the graft structure composed of a carbon–carbon backbone and multiple oligo(ethylene glycol) side chains is different from the standard linear PEG, these

* Corresponding author. Tel.: +1 718 982 3897; fax: +1 718 982 3910.
E-mail address: shuiqin.zhou@csi.cuny.edu (S. Zhou).

0032-3861/$ – see front matter © 2010 Elsevier Ltd. All rights reserved.
doi:10.1016/j.polymer.2010.06.030

nonlinear PEG analogues are mainly composed of oligo(ethylene glycol) segments and are, in most cases, water-soluble and biocompatible [25]. Hence, these thermosensitive nonlinear PEG analogue polymers are very promising for biomedical applications.

Based on the free radical precipitation polymerization technique used to synthesize PNIPAM microgels, Hu's group has successfully synthesized monodisperse copolymer microgels from the comonomers of MEO_2MA and MEO_9MA at different ratios [29]. With the same two-step polymerization method used for the preparation of PNIPAM-based core-shell microgels, they also successfully synthesized core-shell microgels with the poly[oligo(ethylene glycol) ethyl ether methacrylate ($M_n = 246$ g/mol, EEO_3MA)] as core and the copolymer of EEO_3MA, MEO_5MA ($M_n = 300$ g/mol) and acrylic acid as shell. Similar to PNIPAM microgels, these nonlinear PEG analogue polymer microgels can self-assemble into interesting colloidal crystalline phases, depending on the concentration and temperature [30].

The aim of this work is to develop a series of monodisperse oligo (ethylene glycol)-based temperature sensitive core-shell microgels with different shell thickness, and study their potential application as delivery vehicles of hydrophobic drugs. The structures and volume phase transitions of PNIPAM-based core-shell microgels have been well studied [31–34]. The core-shell microgels can provide unique internal structures and multi-responsive properties due to the mutual influence of core and shell swelling, which enables us to explore the possibility to control the uptake and release of drug molecules in the microgels. In our design, the poly [2-(2-methoxyethoxy)ethyl methacrylate] [$P(MEO_2MA)$] microgels with a VPTT ~22 °C is used as a hydrophobic core and the crosslinked copolymer of $P(MEO_2MA\text{-}co\text{-}MEO_5MA)$ with the comonomer ratio of MEO_2MA:MEO_5MA = 1:2 and a VPTT of ~55 °C is used as a hydrophilic shell. In addition to the good biocompatibility, the hydrophilic $P(MEO_2MA\text{-}co\text{-}MEO_5MA)$ shell can influence the core swelling. Although the free $P(MEO_2MA)$ core chain network is hydrophobic and collapsed at temperature above its VPTT, the addition of hydrophilic shell can mechanically expand the collapsed core. As the shell thickness increases to certain extent, the hydrophobic core network can be almost fully expanded even at temperature above the VPTT of core microgels [33,34]. We expect that the hydrophobic core with an open network structure should load hydrophobic drug molecules much more effectively compared to the collapsed structure. To demonstrate this conception, a hydrophobic drug dipyridamole (DIP) (see Scheme 1) was studied as model drug. The effects of shell thickness and temperature on the drug loading efficiency were investigated. The sustained drug release behavior and cytotoxicity of the drug-free/drug-loaded microgels were evaluated. The results presented in this work provide important guidelines for the rational design of biocompatible PEG analogue-based core-shell microgels for drug delivery vehicles.

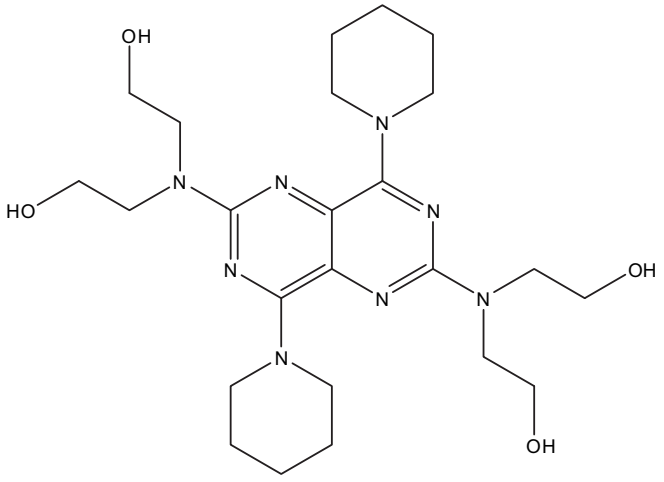

Scheme 1. Chemical structure of model drug DIP.

2. Experimental

2.1. Materials

All reagents were purchased from Sigma–Aldrich. 2-(2-methoxyethoxy)ethyl methacrylate (MEO_2MA, 95%), oligo(ethylene glycol)methyl ether methacrylate ($M_n = 300$ g/mol, MEO_5MA), and poly(ethylene glycol) dimethacrylate (PEGDMA, $M_n \approx 550$ g/mol, crosslinker) were purified with neutral Al_2O_3. Dipyridamole (DIP), sodium dodecyl sulfate (SDS) and ammonium persulfate (APS) were used as received.

2.2. Synthesis of oligo(ethylene glycol)-based core-shell microgels

The $P(MEO_2MA)$ core microgels were respectively synthesized according to the compositions listed in Table 1. Typically, the monomers, PEGDMA crosslinker, and SDS (5.0×10^{-5} mol) were dissolved in 200 mL deionized water. The mixture was heated to 70 °C under a N_2 purge. After 1 h, APS (3.0×10^{-4} mol) was added to the solution to initiate the polymerization. The reaction was allowed to proceed for 5 h. The obtained core microgels were purified by centrifugation (Thermo Electron Co. SORVALL® RC-6 PLUS superspeed centrifuge), decantation, and redispersion in deionized water for three cycles to remove the unreacted small molecules and SDS surfactant molecules. The size of the core microgels is controllable by varying the amount of SDS.

The $P(MEO_2MA\text{-}co\text{-}MEO_5MA)$ shell was synthesized using core microgel particles as nuclei for subsequent precipitation polymerization. The shell precursors of MEO_2MA and MEO_5MA monomer mixture in 1:2 M ratio, PEGDMA crosslinker, and SDS were dissolved in deionized water (for details see Table 1), then the core microgels were added. The mixture was heated to 70 °C under a N_2 purge. After 1 h, the APS initiator was added to start the polymerization. The synthesis was allowed to proceed for 5 h. The resulted core-shell microgels were purified with centrifugation/redispersion in water for three cycles, followed by 3 days of dialysis (Spectra/Por® molecularporous membrane tubing, cutoff 12000–14000) against very frequently changed water at room temperature (~22 °C).

2.3. Drug uptake experiments

8 mL DIP solution (0.5 mg/mL, pH = 2.0) was added into the 10 mL microgel suspensions at a core microgel concentration of 1.0 mg/mL, resulting in a final pH around 3. After being stirred for 20 min, the pH of the mixture was adjusted to 8.0 by an addition of

Table 1
Feeding compositions for synthesis of the core-shell microgels.

Sample	Core Solution (mol)		Shell Solution (mol)		
	MEO_2MA	PEGDMA (550)	MEO_2MA	MEO_5MA	PEGDMA (550)
Core microgel	0.0008	0.8×10^{-5}			
Shell microgel			0.001	0.002	0.3×10^{-4}
CSM1	0.0008	0.8×10^{-5}	0.001	0.002	0.3×10^{-4}
CSM2	0.0008	0.8×10^{-5}	0.002	0.004	0.6×10^{-4}
CSM3	0.0008	0.8×10^{-5}	0.004	0.008	1.2×10^{-4}
CSM4	0.0008	0.8×10^{-5}	0.008	0.016	2.4×10^{-4}

NaOH solution and the mixture was continuously stirred overnight. The DIP–microgel complexes were then removed from suspension by ultracentrifugation at 20,000 rpm and 22 °C for 40 min and redispersed in 10 mL of pH = 8.0 NaOH solution. The supernatant solution of residual DIP was collected and dissolved adequately with 0.1 N HCl to form uniform solution with a final pH being controlled at 3. The concentrations of the residual DIP were determined by fluorescence emission intensity at 480 nm with the excitation wavelength of 414 nm [36–38], based on the linear calibration curve with $R^2 > 0.99$ measured using the DIP solutions with known concentrations under the same condition. The excitation at 414 nm gives an intensive emission band at 480 nm, which allows the detection of DIP in the nanomolar range based on the calibration curve. The drug loading efficiency of microgels was calculated as follows:

$$\text{Drug loading efficiency}(\%) = 100\left(W_{\text{feed drug}} - W_{\text{free drug}}\right)\Big/W_{\text{feed drug}}$$

2.4. In vitro drug release

The release of model drug from the microgel was evaluated by the dialysis method [36,39]. The purified DIP-loaded microgel dispersions (1 mL) were transferred into dialysis tubes with a molecular weight cutoff of 12000–14000 and then immersed into 100 mL 0.005 M phosphate buffer solutions at different pHs. The aliquots outside of the dialysis bag were sampled at time intervals. The released drug concentrations were assayed using the fluorescence spectrometry for DIP, as outlined for the drug uptake measurements. Cumulative release is expressed as the total percentage of drug released through the dialysis membrane over time.

2.5. In vitro cytotoxicity

Mouse melanoma cells B16F10 (2000 cell/well) were cultured in DMEM containing 10% FBS and 1% penicillin–streptomycin in a 96-well plate, and exposed to free DIP, DIP-free microgels, and DIP-loaded microgels. To cover the high concentrations, the microgels were concentrated and adjusted to an appropriate concentration in DMEM right before feeding into the well. The plate was incubated at 37 °C for 2 h. The medium was then aspirated, and these wells were washed using fresh serum-free DMEM. After that, 25 μL of 3-(4,5-dimethyl-2-thiazolyl)-2,5-diphenyltetrazolium bromide (MTT) solution (5 mg/mL in PBS) were added to the wells. After incubation for 2 h, the solution was aspirated and 100 μL of DMSO was added to each well to dissolve the formazan crystal, and the plate was sealed and incubated overnight at 37 °C with gentle mixing. Cell viability was measured using a microplate reader at 570 nm. Positive controls contained no drug or microgels, and negative controls contained MTT. Results are expressed as a percentage of the absorbance of the positive control.

2.6. Characterization

The morphology of the core-shell microgels was characterized with transmission electron microscopy (TEM). The TEM images were taken on a Zeiss EM 902 transmission electron microscope operating at an accelerating voltage of 100 kV. Approximately 10 μL of the diluted microgel suspension was dropped on a Formvar-covered copper grid (300 meshes) and then air-dried at room temperature for the TEM measurements. The PL spectra were obtained on a JOBIN YVON Co. FluoroMax®-3 Spectrofluorometer equipped with a Hamamatsu R928P photomultiplier tube, calibrated photodiode for excitation reference correction from 200 to 980 nm. The pH values were obtained on a METTLER TOLEDO SevenEasy pH meter.

The size and size distribution of the microgels under different conditions were measured using a standard light scattering spectrometer (BI-200SM) equipped with a BI-9000 AT digital time correlator (Brookhaven Instrument, Inc.). A He–Ne laser (35 mW, 633 nm) was used as the light source. The diluted microgel dispersion solutions were passed through 0.45 μm Millipore Millex-HV filters to remove dust. In dynamic light scattering, the Laplace inversion of each measured intensity–intensity time correlated function can result in a characteristic line width distribution $G(\Gamma)$ [35]. For a purely diffusive relaxation, Γ is related to the translational diffusion coefficient D by $(\Gamma/q^2)_{C\to 0,q\to 0} = D$, where $q = (4\pi n/\lambda)\sin(\theta/2)$ with n, λ, and θ being the solvent refractive index, the wavelength of the incident light in vacuo, and the scattering angle, respectively. $G(\Gamma)$ can be further converted to a hydrodynamic radius (R_h) distribution by using the Stokes–Einstein equation, $R_h = (k_B T/6\pi\eta)D^{-1}$, where T, k_B, and η are the absolute temperature, the Boltzmann constant, and the solvent viscosity, respectively.

3. Results and discussion

3.1. Synthesis of oligo(ethylene glycol)-based core-shell microgels

Our strategy to prepare the oligo(ethylene glycol)-based core-shell microgels involves the first synthesis of a P(MEO_2MA) core microgel, followed by the synthesis of P(MEO_2MA-*co*-MEO_5MA) gel layer on the core microgel. The P(MEO_2MA) core microgels were synthesized at 70 °C (well above the LCST of P(MEO_2MA)) based on the well-established precipitation polymerization method. Fig. 1 shows the size distributions of the P(MEO_2MA) microgels, in terms of the hydrodynamic radius (R_h) measured at $T = 25$ °C and $\theta = 45°$, synthesized with different concentrations of SDS surfactant. All the obtained P(MEO_2MA) microgel particles have a very narrow size distribution. The DLS characterization indicated that the obtained microgels are nearly monodispersed with a polydispersity index of $\mu_2/\langle\Gamma\rangle^2 = 0.001$. The particle size decreases with the increase in SDS concentration, which enables us to control

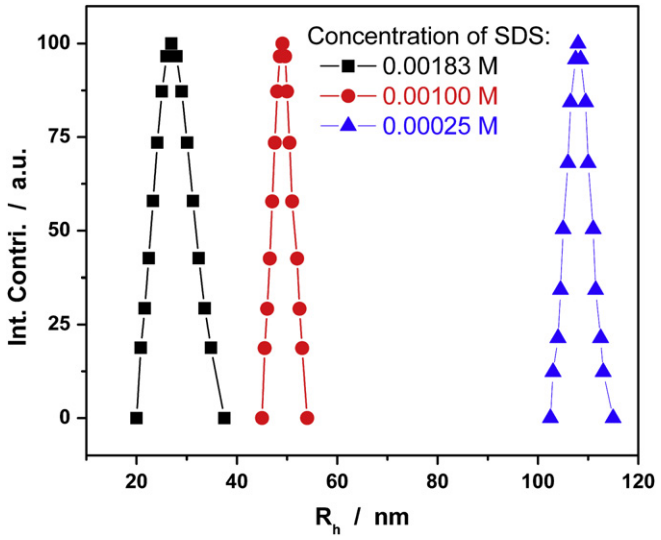

Fig. 1. Size distributions of P(MEO_2MA) core microgels synthesized with different SDS concentrations, measured at 22 °C and a scattering angle of $\theta = 45°$.

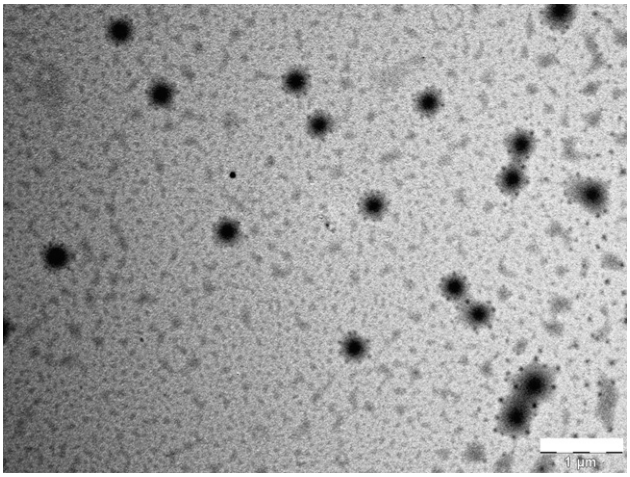

Fig. 2. Typical TEM image of the core-shell microgels (CSM3). The citric acid-capped gold nanoparticles are attached onto the shell surface for easy visualization of the core-shell structure. The scale bar is 1 μm.

the size of core microgel by a simple change in the amount of surfactant as the application needs. For the P(MEO_2MA) core microgels, the hydrodynamic diameter below 100 nm can be easily obtained in the presence of small amount of SDS (e.g., 1–2 mM, well below the critical micelle concentration of SDS). The P(MEO_2MA) microgels with R_h = 110 nm at 22 °C was chosen as core model for the further synthesis of core-shell microgels using the method developed by Lyon's group [31].

The further synthesis of P(MEO_2MA-*co*-MEO_5MA) gel shell was performed at 70 °C, at which the P(MEO_2MA) core microgels are fully collapsed. The collapsed core cannot only serve as nuclei for further polymerization of shell, resulting in preferential growth of the existing particles over the nucleation of new ones, but also prevent the penetration of shell polymer into the core area [31a]. Fig. 2 shows the typical TEM image of dried core-shell microgels CSM3 (see Table 1). The resulted core-shell microgels have a clear boundary between the core and shell. The core-shell structure can be clearly observed with a dark condensed core and a light contrast shell. The low contrast of shell is due to the highly swollen state of the P(MEO_2MA-*co*-MEO_5MA) gel layer at sample preparation temperature. To observe the low contrast shell, the microgel suspension was mixed with citric acid-capped gold nanoparticles (~33 nm). The gold nanoparticles can be readily anchored onto the surface of microgels through the hydrogen bonding between the –COOH groups and the ethylene oxide (EO) units. It is clear that the gold nanoparticles anchored on the shell region give us an easy visualization of the whole core-shell microgel particles. On the basis of the core-shell structure as demonstrated, the thickness of shell can be controlled by adding different amount of shell monomers relative to a fixed amount of core particles. This is similar to the synthesis of PNIPAM-based core-shell microgels [33].

3.2. Temperature-responsive volume phase transitions of the core-shell microgels

Fig. 3A shows the thermo-responsive volume phase transitions of the core microgels of P(MEO_2MA) and the pure shell-composed microgels of P(MEO_2MA-*co*-MEO_5MA), respectively. The volume phase transition of core microgels begins around 13 °C. The core microgels are nearly collapsed at room temperature, and completely collapsed at body temperature. In contrast, the shell-composed P(MEO_2MA-*co*-MEO_5MA) microgels show a very broad transition temperature beginning at around 40 °C. However, at the experimental temperature limit of ~55 °C, the shell-composed microgels still have not reached the collapsing limit. Thus, the shell-composed microgels are highly swollen and very hydrophilic at the temperatures below 40 °C.

Fig. 3B shows the temperature-dependent average R_h of the four core-shell microgels. Two features should be noted. Firstly, the increase in the feeding amount of shell components increases the thickness of the resultant shells. The size difference between the core-shell microgels and the parent core microgels can be attributed to the shell layer. Thus the thickness of the shell was estimated for the core-shell microgels. For example, at 7.5 °C, the increase of R_h from 157 nm for the core microgel to 165 nm (CSM1), 176 nm (CSM2), 190 nm (CSM3) and 256 nm (CSM4), respectively, corresponds to a shell thickness of 8 nm, 19 nm, 33 nm, and 99 nm. Secondly, the core-shell microgels with different shell thickness exhibited different volume phase transition temperatures (VPTT). The increase in shell thickness shifts the VPTT of the core microgels toward higher temperatures, which is consistent with the results observed in the PNIPAM-based core-shell microgels [31–33]. For CSM1 and CSM2 with thinnest shells, these microgels start to shrink at temperature above 15 °C, which is slightly higher than the VPTT of the core microgels. When the shell thickness is increased to 33 nm, the CSM3 microgels begins to shrink around 24 °C, indicating a shift of the VPTT of core with 11 °C higher compared to the core microgels. For the CSM4 microgels with the thickest shell of 99

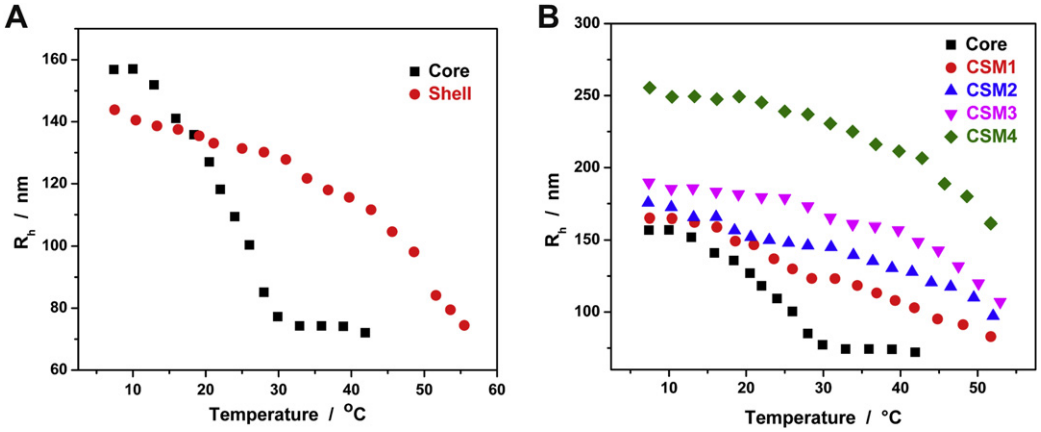

Fig. 3. (A) Average R_h values of P(MEO_2MA) core and P(MEO_2MA-*co*-MEO_5MA) shell microgels as a function of temperature, respectively, measured at $\theta = 45°$. (B) Temperature dependence of average R_h values of core-shell microgels with different shell thickness, respectively, measured at $\theta = 45°$. The parent core is shown for comparison.

nm, no significant volume phase transition was observed within the experimental temperature range, indicating that the phase behavior of the CSM4 microgels is almost similar to that of the pure shell-composed microgels of P(MEO_2MA-*co*-MEO_5MA), in terms of VPTT.

In addition to the VPTT shift, the shell thickness can also dramatically affect the collapsing degree of the core region in the core-shell microgels. As temperature increased from 10 to 32 °C, the full collapse of the free core microgels resulted in a decrease of 83 nm in R_h, while the R_h of the CSM1, CSM2, CSM3, and CSM4 only reduced 42, 28, 20, and 18 nm, respectively. Obviously, the shell can significantly restrict the shrinking of the core at the elevated temperature. The thicker the shell is, the less the collapsing degree of core network has. It was known that the swelling behavior of a core-shell microgel is not a simple addition of the individual core and shell components. The mutual interaction between the shell and the core has been studied for PNIPAM-based core-shell microgels [31–33]. In our systems, at temperatures below the VPTT (e.g., <40 °C) of the core-shell microgels, the hydrophilic shell will try to maintain its swollen state (Fig. 3A). Although water is a poor solvent for the P(MEO_2MA) core network chains at temperature above 30 °C, the thick and swollen P(MEO_2MA-*co*-MEO_5MA) copolymer gel shell will mechanically pull up the lightly crosslinked core network. The final equilibrium collapsing degree of the core networks in the core-shell microgels depends on the counterbalance of the expanding (hydrophilic shell) and retracting forces (hydrophobic core). Under this consideration, it allows us to control the collapsing degree (mesh size of network) of the hydrophobic core simply by tailoring the thickness of the shell. When modified with a P(MEO_2MA-*co*-MEO_5MA) gel shell of sufficient thickness, it is expected that the hydrophobic P(MEO_2MA) core networks can be stretched up to nearly a full expansion even at the high temperatures above the VPTT of the core but below that of the shell-composed microgels, e.g., 40 °C. Indeed, the collapsing degree ($R_{h,40\ °C}/R_{h,10\ °C} = 0.84$) of the CSM4 microgels with the thickest shell of 99 nm is nearly the same as that ($R_{h,40\ °C}/R_{h,10\ °C} = 0.82$) of pure shell-composed microgels, which indicates that the core in CSM4 microgels has no contribution to the size reduction of the CSM4 microgels in this specific temperature range and the core is almost fully expanded. This unique shell thickness-dependent collapsing degree of the hydrophobic core in our core-shell microgels is a key parameter for the storage and delivery of hydrophobic drugs, because the equilibrium collapsing degree (or mesh size) influences the loading capacity and drug diffusion coefficient.

3.3. Drug loading efficiency of the P(MEO_2MA-co-MEO_5MA) core-shell microgels

The hydrophobic P(MEO_2MA) core of our core-shell microgels offer the capability for storage of hydrophobic drugs. DIP was chosen as the model drug. DIP is a known platelet inhibitor, coronary vasodilator [40] and a coactivator of antitumor compounds [41,42]. As a poor soluble weak base with a reported pKa of 6.4, the solubility of DIP can be significantly different in different digestive fluids. For example, DIP dissolves readily in the stomach but incompletely in the intestine. Therefore, an effective carrier for such a drug is required.

Fig. 4 shows the effect of shell thickness on the drug loading efficiency of the core-shell microgels measured at a constant number concentration of microgel particles together a fixed feeding concentration of drug and 22 °C. It is clear that the loading efficiency increases with the increase in shell thickness, and then reaches a nearly plateau slope, which indicates that the loading efficiency only increases slightly with the further increase in shell

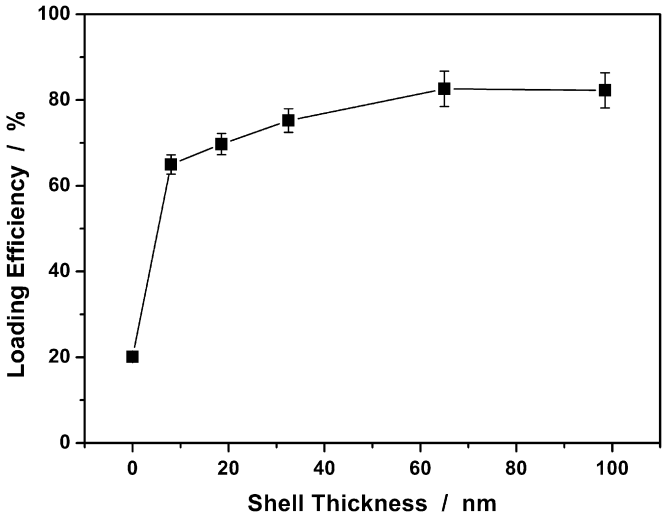

Fig. 4. DIP loading efficiency of the core-shell microgels as a function of shell thickness, measured at a fixed number concentration of microgel particles and 22 °C.

thickness after the shell thickness reaches a certain value. These results imply that the shell may contribute very little to the overall drug loading. Control experiment confirmed that the pure shell-composed microgels of P(MEO_2MA-*co*-MEO_5MA) did show an extremely low loading capacity of 8.5 mg DIP/g dry microgel. Although the free P(MEO_2MA) core microgels also demonstrate a low drug loading efficiency with 20% for DIP (equivalent to 80.5 mg DIP/g dry microgel), which is still one order of magnitude higher in loading capacity than the pure shell-composed microgels. Therefore, the loading of DIP into the core-shell microgels mainly depends on the hydrophobic interactions [36,43] between the drug and the P(MEO_2MA) core.

Upon demonstrating the important role of the hydrophobic interactions in DIP loading, it is noteworthy that the free P(MEO_2MA) core microgels, when compared with the core-shell microgels, still exhibit low loading efficiency. We speculate that the collapsing degree (mesh size of network) of the hydrophobic core is another important factor related to the drug loading capacity. The low loading efficiency of the free core microgels could be attributed to their fully collapsed structure. The core microgels is nearly collapsed at 22 °C and the P(MEO_2MA) network chains are hydrophobic and densely sticked together. Such a collapsed structure has limited space to hold the drug molecules. The core-shell structure can increase the drug loading efficiency dramatically. As we have discussed above (Fig. 3B), the hydrophilic and swollen shell layer can restrict the collapsing of the P(MEO_2MA) core. Although the P(MEO_2MA) core network chains are still very hydrophobic, but the swollen shell will pull up and stretch the core network. In such a case, the hydrophobic core has open network with large mesh size for drug molecules diffusing into the core area. The thicker swollen shell has larger pulling force to prevent the collapsing of the hydrophobic core network chains, thus the mesh size of the core in CSM2 and CSM3 is larger than those of CSM1 and parent core at 22 °C, which can hold more hydrophobic drug molecules in the interior of the hydrophobic core. When the shell thickness is increased to a certain value, the mesh size of the hydrophobic core network chains will no longer increase due to the limitation of chemical crosslinking, thus the loading capacity of the core can reach to a maximum and the overall loading efficiency of the core-shell microgels can only increase very slightly with further increase in shell thickness due to the very low loading capacity of shell (Fig. 4). Therefore, certain shell thickness in the core-shell microgels is necessary to achieve maximum drug loading.

The hypothesis can be further supported by the temperature effect on the drug loading efficiency. Fig. 5 shows the DIP loading efficiency of the CSM2 and CSM3 core-shell microgels at different temperatures. At the temperature window of between the VPTT of the core microgels and the shell-composed microgels (e.g. 22–40 °C, Figs. 3A and 5), the hydrophilic shell restricts the collapse of core network chains, which can maintain the mesh size of hydrophobic core to hold hydrophobic drug molecules. As a consequence, the loading efficiency for drug molecules remains nearly a constant. When the temperature is further increased (>40 °C), the shell will continuously shrink and gradually becomes hydrophobic, thus both hydrophobic core and partial hydrophobic shell layer can hold hydrophobic drug molecules, and a higher loading efficiency can be expected. However, when temperature is increased to ~65 °C, a dramatic decrease in drug loading efficiency was observed. Although both core and shell are very hydrophobic to interact with hydrophobic drug molecules, the shell is collapsed and loses its function for pulling up the network at such a high temperature, resulting in a collapsed P(MEO_2MA) core without the restriction of swollen shell. The very small mesh size of both core and shell gel limits the loading amount of drug molecules. Clearly, in addition to the drug–polymer hydrophobic interactions, the mesh size of the hydrophobic core is also very important to determine the loading capacity of hydrophobic drugs. These results indicate that the temperature range between the VPTT of core microgels and the shell-composed microgels is the most suitable condition to achieve high loading efficiency of hydrophobic drugs.

3.4. In vitro release studies

Fig. 6 shows the cumulative release profiles of DIP from the CSM2 core-shell microgels to buffer solutions at different pH values and 22 °C. It was anticipated that the drug molecules trapped in the hydrophobic core could gradually diffuse into the hydrophilic shell and then diffuse out of the shell to be released. At pH = 7.4, only ~14% of the loaded DIP can be released after 28 h. When the pH was decreased to 3, ~35% of the loaded DIP can be released after 25 h due to the partial protonation of DIP. The results were further analyzed to understand the release mechanism of the drug release from the core-shell microgels. The analysis was performed on the basis of the empirical equation proposed by Peppas et al. [44]:

$$M_t/M_\infty = kt^n$$

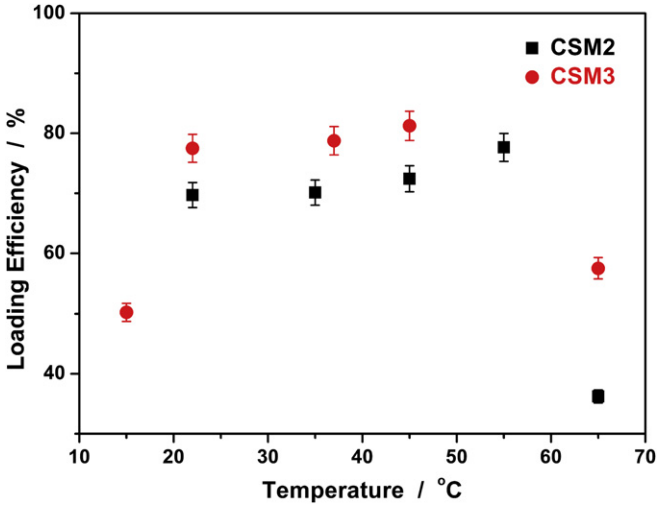

Fig. 5. The temperature dependence of the DIP loading efficiency of the core-shell microgels CSM2 and CSM3.

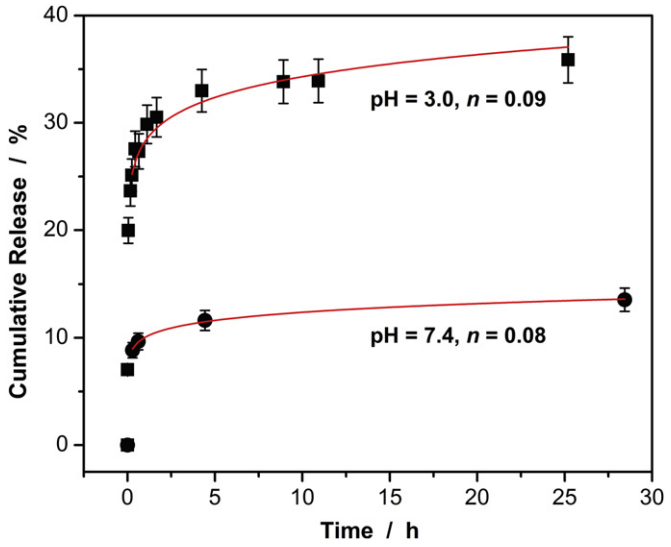

Fig. 6. Cumulative DIP release from the core-shell microgels (CSM2) to buffer solutions at different pH values and 22 °C.

where M_t and M_∞ is the amount of drug released up to any time t and the final amount of drug; k is a structural/geometric constant and n is a release exponent related to the intimate mechanism of release. The power law is easy to use and can be applied to most diffusion-controlled release systems, even if it is too simple to offer a robust prediction for complicated release phenomena. The advantage of this approach is that it yields a convenient measure of the constancy of release rate in the value of n. It also provides a quick way to check the releasing mechanisms, as values of $n < 0.43$ or $n > 0.85$ for spheres or sphere-like device indicate another controlling process in addition to the diffusion process.

The n values presented in Fig. 6 are obtained from the best fitting of our experimental curves. DIP is soluble at pH = 3.0, but the unionized DIP molecules have a very low water solubility ($\leq 5 \times 10^{-6}$ g/mL) at pH = 7.4 [45,46]. Despite of the difference in the solubility of DIP, the exponent n was found to be nearly the same at the two-pH values. The low n values exclude the simple diffusion-controlled delivery mechanism. The investigated pH variable affects the release rate, but essentially does not change the drug release mechanism. These results confirm that the release of DIP molecules trapped in the core-shell microgels obeys to two correlated processes within the delivery matrix. One is related to the interactions between the drug and polymer chains, including the hydrophobic associations between DIP molecules and the hydrophobic backbone chains as well as the hydrogen bonding between the hydroxyl groups of the DIP molecules and the ether oxygen of the ethylene glycol units. Another is a diffusion-controlled step. It should be noted that the prepared microgels are very stable. The drug loading/releasing test for a week has nearly no effect on the thermo-responsive volume phase transitions of the core-shell microgels within the experimental errors (see Supporting information), which indicates that the degradation occurred on the drug carriers should be negligible during the drug release time.

3.5. In vitro cytotoxicity

For future biological applications, materials should be non- or low-cytotoxic. To evaluate the cytotoxicity of the core-shell microgels, *in vitro* cytotoxicity tests were conducted against mouse melanoma B16F10 cells. As shown in Fig. 7, the empty core-shell

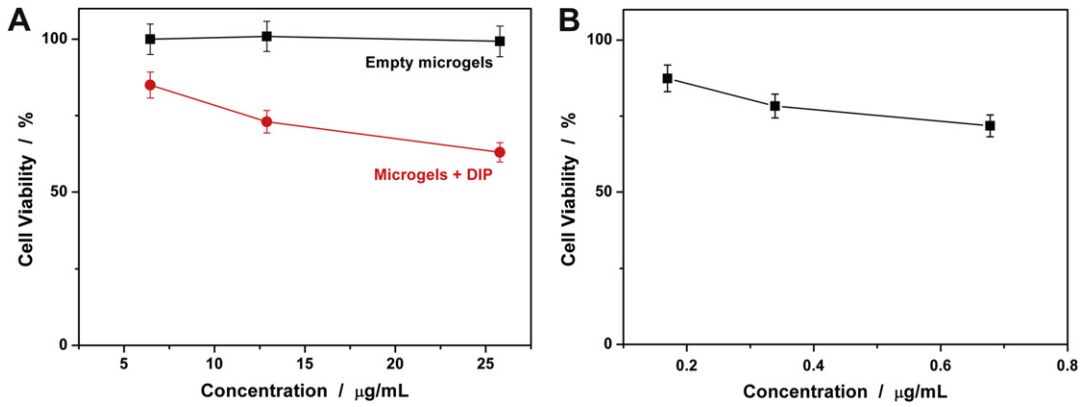

Fig. 7. (A) In vitro cytotoxicity of empty CSM3 microgels, and DIP-loaded microgels against B16F10 cells. (B) The control experiment on the free DIP solution was presented for comparison. The concentrations of DIP used for the control study are equal to DIP-loaded in the interior of the CSM3 microgels correspondingly.

microgels were non-cytotoxic to B16F10 cells in concentrations of upto 25.8 μg/mL. These results indicate that our microgels based on the oligo-(ethylene glycol) macromonomers exhibit an excellent *in vitro* biocompatibility. In contrast, when the cells were exposed to DIP, the cell viability drastically decreased. Likewise, an even higher cell death was observed in cells treated with DIP-loaded microgels (containing equivalent amount of DIP to free DIP). When the cells were incubated with DIP-loaded microgels even at a concentration as low as 6.44 μg/mL (equivalent to about 0.17 μg/mL free DIP), the cell viability drastically decreased, which indicates that the DIP-loaded microgels can interact with cells and are pharmacologically active. DIP is a known coactivator of antitumor compounds, and the formation of metastatic tumors could be inhibited by such inhibitors of platelet aggregation [41]. Despite of these encouraging preliminary results and a compelling biochemical rationale, we cannot conclude whether the DIP drug would be pharmacologically active for cancer treatment because very limited information exists on the clinical use of anticoagulants for the prevention or treatment of cancer [42]. Nevertheless, the increase in cytotoxicity in the presence of DIP-loaded microgels can be attributed to the cellular uptake of DIP-loaded microgels and possibly their sustained-release property.

4. Conclusion

Well-defined oligo(ethylene glycol)-based doubly thermosensitive core-shell microgels with the P(MEO_2MA) microgel as a hydrophobic core and the P(MEO_2MA-*co*-MEO_5MA) gel layer as a hydrophilic shell could be successfully synthesized via precipitation polymerization. The presence of P(MEO_2MA-*co*-MEO_5MA) hydrophilic shell could prevent the hydrophobic core network from collapsing, resulting in a shift of the VPTT of P(MEO_2MA) core to higher temperatures in comparison with the free parent core microgels. The simple synthesis also allows us to tailor the shell layer to different thickness. When the shell thickness is increased to a certain extent (e.g., $\geq$50 nm), the hydrophobic core network can be fully expanded. This unique structure of hydrophobic core with the open network (or large mesh size) in the core-shell microgels can dramatically improve the loading capacity for hydrophobic drugs, which indicates that both the drug-core hydrophobic interactions and the mesh size of core networks are important to determine the drug loading efficiency. These nontoxic core-shell microgels provide well-controlled drug loading yield and sustained drug release profiles. The DIP-loaded core-shell microgels significantly enhanced the *in vitro* cytotoxicity against tumor cells in comparison with the equivalent amount of free DIP molecules in solution. Although DIP was selected as a specific model drug in this study, the concept and technique of developing nontoxic polymeric drug carriers by loading drug molecules into polymer chain networks through stimuli-responsive gel engineering can be generalized to deliver many other types of therapeutic or diagnostic agents.

Acknowledgements

We gratefully acknowledge the financial support of this work by the US Agency for International Development under the US–Pakistan Science and Technology Cooperative Program (PGA-P280422) and PSC-CUNY research award. We thank Prof. Probal Banerjee for his training on the cytotoxicity test experiments.

Appendix. Supporting information

Supplementary data associated with this article can be found, in the online version, at doi:10.1016/j.polymer.2010.06.030.

References

[1] Das M, Zhang H, Kumacheva E. Annu Rev Mater Res 2006;36:117–42.
[2] Malmsten M. Soft Matter 2006;2:760–9.
[3] Oh JK, Drumright R, Siegwart DJ, Matyjaszewski K. Prog Polym Sci 2008;33:448–77.
[4] Saunders BR, Laajam N, Daly E, Teow S, Hu X, Stepto R. Adv Colloid Interface Sci 2009;147–8:251–62.
[5] Das M, Mardyani S, Chan WCW, Kumacheva E. Adv Mater 2006;18:80–3.
[6] Thienen TG, Raemdonck K, Demeester J, De Smedt SC. Langmuir 2007;23:9794–801.
[7] Shi L, Khondee S, Linz TH, Berkland C. Macromolecules 2008;41:6546–54.
[8] Ghugare S, Mozetic P, Paradossi G. Biomacromolecules 2009;10:1589–96.
[9] Nolan CM, Serpe MJ, Lyon LA. Biomacromolecules 2004;5:1940–6.
[10] Das M, Sanson N, Fava D, Kumacheva E. Langmuir 2007;23:196–201.
[11] Nolan CM, Reyes C, Debord J, Garcia A, Lyon LA. Biomacromolecules 2005;6:2032–9.
[12] Nolan C, Gelbaum LT, Lyon LA. Biomacromolecules 2006;7:2918–22.
[13] Snowden MJ. J Chem Soc Chem Commun 1992;11:803–4.
[14] Huo D, Li Y, Kobayashi T. Adv Mat Res 2006;11-12:299–302.
[15] Wu JY, Liu SQ, Heng PW, Yang YY. J Controlled Release 2005;102:361–72.
[16] Zhou J, Wang G, Zou L, Tang L, Marquez M, Hu Z. Biomacromolecules 2008;9:142–8.
[17] Hoare T, Pelton R. Langmuir 2008;24:1005–12.
[18] Pelton R. Adv Colloid Interface Sci 2000;85:1–33.
[19] Castro-Lopez V, Hadgraft J, Snowden MJ. Int J Pharm 2005;292:137–47.
[20] Zhang Y, Guan Y, Zhou S. Biomacromolecules 2007;8:3842–7.
[21] Harsh DC, Gehrke SH. J Controlled Release 1991;17:175–85.
[22] Lutz JF, Hoth A. Macromolecules 2006;39:893–6.
[23] Lutz JF, Akdemir O, Hoth A. J Am Chem Soc 2006;128:13046–7.
[24] Lutz JF, Weichenhan K, Akdemir O, Hoth A. Macromolecules 2007;40:2503–8.
[25] Lutz JF. J Polym Sci Part A Polym Chem 2008;46:3459–70.
[26] Han S, Hagiwara M, Ishizone T. Macromolecules 2003;36:8312–9.

[27] Ishiznoe T, Seki A, Hagiwara M, Han S, Yokoyama H, Oyane A, et al. Macromolecules 2008;41:2963–7.
[28] Badi N, Lutz JF. J Controlled Release 2009;140:224–9.
[29] Cai T, Marquez M, Hu Z. Langmuir 2007;23:8663–6.
[30] Chi C, Cai T, Hu Z. Langmuir 2009;25:3814–9.
[31] (a) Jones CD, Lyon A. Macromolecules 2000;33:8301–6;
(b) Jones CD, Lyon A. Macromolecules 2003;36:1988–93;
(c) Jones CD, Lyon A. Langmuir 2003;19:4544–7.
[32] (a) Gan D, Lyon A. J Am Chem Soc 2001;123:8203–9;
(b) Jones CD, McGrath JG, Lyon A. J Phys Chem B 2004;108:12652–7.
[33] Berndt I, Richtering W. Macromolecules 2003;36:8780–5.
[34] Berndt I, Pedersen JS, Lindner P, Richtering W. Langmuir 2006;22:459–68.
[35] Chu B. Laser light scattering. 2nd ed. New York: Academic Press; 1991.
[36] Tang Y, Liu SY, Armes SP, Billinghan NC. Biomacromolecules 2003;4:1636–45.
[37] Giacomelli C, Le ML, Borsali R, Lai-Kee-Him J, Brisson A, Armes SP, et al. Biomacromolecules 2006;7:817–28.
[38] Vertzoni M, Pastelli E, Psachoulias D, Kalantzi L, Reppas C. Pharm Res 2007;24:909–17.
[39] Jiang X, Ge Z, Xu J, Liu H, Liu S. Biomacromolecules 2007;8:3184–92.
[40] Marchandt E, Prichard AD, Casanegra P, Lindsay L. Am J Cardiol 1984;53:718.
[41] Shalinsky DR, Jekunen AP, Alcaraz JE, Christen RD, Kim S, Khatibi S, et al. Br J Cancer 1993;67(1):30.
[42] Hejna M, Raderer M, Zielinski CC. J Natl Cancer Inst 1999;91:22.
[43] KozlovYu M, Melik-Nubarov NS, Batrakova EV, Kabanov AV. Macromolecules 2000;33:3305.
[44] Siepmann J, Peppas NA. Adv Drug Deliv Rev 2001;48:139.
[45] Giacomelli C, Schmidt V, Borsali R. Langmuir 2007;23:6947–55.
[46] Avdeef A, Berger CM, Brownell C. Pharm Res 2000;17:85–9.